The Dioxoosmium(VI) Complex $[OsO_2(H_2biim)_2](NO_3)_2$ as Oxygen-Transfer Reagent − Synthesis and Solid-State Structure of Bis(2,2′-biimidazole)-bis(triphenylphosphane oxide)osmium(III) Nitrate

Andrei Maiboroda,[a] Gerd Rheinwald,[a] and Heinrich Lang*[a]

Dedicated to Prof. D. Sellmann on the occasion of his 60th birthday

Keywords: Coordination chemistry / Osmium / N ligands / Oxygen transfer / X-ray structure analysis

Treatment of OsO_4 (**1**) with 2,2′-biimidazole (H_2biim) (**2**) in a methanol/acetone mixture, and in the presence of nitric acid produces the novel dioxoosmium(VI) complex $[OsO_2(H_2biim)_2](NO_3)_2{\cdot}CH_3OH$ (**3**). Addition of 2 equiv. of PPh_3 (**4**) and 1 equiv. of nitric acid to **3** affords mononuclear $[Os(H_2biim)_2(O{=}PPh_3)_2](NO_3)_3$ (**5**) by a redox reaction which involves the transfer of oxygen from osmium to PPh_3. The X-ray crystal structure of **5** reveals an octahedral coordination sphere around the osmium(III) centre. This occurs as a result of the two H_2biim chelating ligands in the equatorial positions and two datively bonded phosphane oxide groups O=PPh_3 in the axial positions. Hydrogen bonds are responsible for the formation of a polymeric structure in the solid state. The latter complex reacts with KOH to form monocationic $[Os(Hbiim)_2(O{=}PPh_3)_2]NO_3$ (**6**).

Introduction

Platinum metal containing complexes with, for example, five-membered nitrogen-containing heterocycles are of considerable interest since they can be used as starting materials for the synthesis of oligo- and polymetallic species, featuring at least two different metal centres.[1,2] Representative examples of such species are the pyrazolato-bridged homobimetallic rhodium and iridium complexes $[\{Rh_2(\mu\text{-}pz)_2(I)(C{\equiv}NtBu)_4\}_2(\mu\text{-}I)](CF_3SO_3)$,[1b] $[M(\mu\text{-}pz)(I)(C{\equiv}NtBu)_2]_2$,[1b] (M = Rh, Ir) and $Ir_2(\mu\text{-}H)(\mu\text{-}pz)(N{\equiv}CMe)(PiPr_3)_2$[2b] (pz = pyrazolate). In these complexes, the nitrogen-containing heterocyclic π-conjugated bridging units span the corresponding transition metal centres, giving rise to a bonding situation which allows the metal atoms to communicate with each other.[1] A further common feature of oligo- or polymetallic complexes is their significantly higher activity in many homogeneous catalytic processes, e.g. hydrogenation, hydroformylation, compared with their predecessors.[2] This catalytic enhancement can be explained in terms of an intramolecular electron transfer between the corresponding transition metal centres, via the π-conjugated organic building blocks.[3] Hence, the development of the chemistry of azolato-containing transition metal complexes of platinum metals is of interest, either in homogeneous catalysis, due to cooperative and synergetic effects, or in the study of intramolecular electronic communication.

For the synthesis of osmium complexes bearing 2,2′-biimidazole chelating ligands, the hydrido(phosphane) complexes $OsH_2Cl_2(PiPr_3)_2$[4a] or $OsH_6(PiPr_3)_2$[4b] were exclusively used as the synthetic tool. Nevertheless, all complexes prepared by this method contain only one 2,2′-biimidazole chelating group. Using the 2,2′-biimidazole as the bridging unit, also some heterobimetallic complexes, such as $(PiPr_3)_2H_2ClOs(\mu\text{-}Hbiim)MCl(cod)$ (M = Rh, Ir; cod = cyclooctadiene)[4a] or $(PiPr_3)_2H_3Os(\mu\text{-}biim)Ir(cod)$[4b] could also be prepared. Our aim in the present work was to synthesise different osmium complexes, containing at least two 2,2′-biimidazole chelating ligands, so as to use these species as effective starting materials for the preparation of oligonuclear transition metal complexes, based on the central osmium fragments $[Os(biim)_2(O{=}PPh_3)_2]^-$ or $[Os(Hbiim)_2(O{=}PPh_3)_2]^+$. We thus describe the reaction of OsO_4 with H_2biim in order to synthesise neutral and/or ionic osmium complexes, which feature two 2,2′-biimidazole ligands.

Results and Discussion

Synthesis and Spectroscopic Characterisation

In an attempt to synthesise osmium complexes with H_2biim chelating ligands (H_2biim = 2,2′-biimidazole) in the equatorial positions, we chose the dioxoosmium entity as the central building block. OsO_4 (**1**) was treated with two equivalents of H_2biim (**2**), in a 1:1 methanol/acetone mixture, and in the presence of nitric acid to afford the osmium(VI) complex $[OsO_2(H_2biim)_2](NO_3)_2{\cdot}CH_3OH$ (**3**) in a 60% yield (Scheme 1).

---

[a] Technische Universität Chemnitz, Fakultät für Naturwissenschaften, Institut für Chemie, Lehrstuhl für Anorganische Chemie,
Straße der Nationen 62, 09111 Chemnitz, Germany
E-mail: heinrich.lang@chemie.tu-chemnitz.de

1434−1948/01/0909−2263 $ 17.50+.50/0

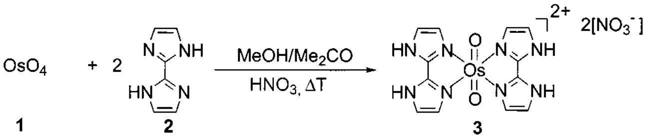

Scheme 1

After appropriate workup, mononuclear **3** was obtained as an air-stable orange solid. However, it was found that **3** is poorly soluble in all well-known organic solvents, except dimethyl sulfoxide. The spectroscopic data (IR, ^1H, $^{13}C\{^1H\}$ NMR spectroscopy) of **3**, in which a planar Os(H_2biim)$_2$ arrangement is present, are consistent with the formulated structure (vide supra).

In the IR spectrum of **3** an intensive absorption band at 858 cm^{-1} is found, which can be assigned to the $\nu_{a(Os=O)}$ stretching vibration of the linear O=Os=O entity.[5] Additionally, a very sharp and narrow $\nu_{(NH)}$ absorption band is observed at 3140 cm^{-1}. As is typical for noncoordinated NO_3^- counter ions, only one band arises at 1488 cm^{-1} which is due to the asymmetric $\nu_{(NO)}$ stretching vibration.[6]

In the noncoordinated state the H_2biim ligand gives rise to only one ^1H NMR resonance signal at $\delta = 7.1$ assigned to the CH protons, whereas in mononuclear **3**, two signals at $\delta = 7.81$ (5-, 5′-H), as well as $\delta = 8.45$ (4-, 4′-H) are observed in a 1:1 intensity ratio. This points to the fact that the H_2biim entity is bonded to the osmium(VI) centre as a chelate, via the two sp^2-hybridised nitrogen atoms; the NH functionalities are located on the opposite side.

Nevertheless, due to the low solubility of **3** in [D$_6$]dimethyl sulfoxide, only the resonance signals for the carbon atoms in the 4,4′- ($\delta = 128.7$) and the 5,5′-position ($\delta = 123.4$) could be detected in the $^{13}C\{^1H\}$ NMR spectrum, which also supports the symmetrical bonding of the H_2biim chelates to the osmium centre.

Dimethyl sulfoxide is the only suitable solvent for **3**, despite its high boiling point and its high coordination ability. It is for this reason that we wanted to prepare complexes with similar structures which are more soluble in common organic solvents, so that we could use these complexes as starting materials in the synthesis of oligometallic transition metal complexes. Therefore, we treated complex **3** with 2 equiv. of Ph_3P (**4**) and 1 equiv. of HNO_3 in boiling tetrahydrofuran containing 10% H_2O. During this reaction, the oxygen atoms bonded to the osmium centre transfer to the phosphorus atom of the added PPh_3. The resulting phosphane oxides $Ph_3P=O$ selectively bond to the osmium centre of the Os(H_2biim)$_2$ segment, through their oxygen atoms in a dative fashion, to produce [Os(H_2biim)$_2$(O=PPh$_3$)$_2$]$^{2+}$ at first. The latter osmium(II) species is the most likely intermediate, which is then oxidised by nitric acid to produce [Os(H_2biim)$_2$(O=PPh$_3$)$_2$](NO$_3$)$_3$ (**5**) in a 76% yield based on **3** (Scheme 2).

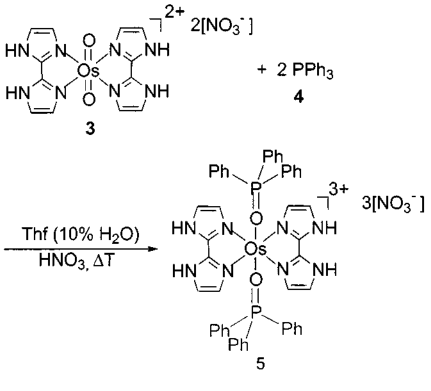

Scheme 2

Complex **5**, when compared with **3**, is significantly more soluble in common organic solvents, such as dichloromethane, methanol, or acetone. However, similar oxygen transfer reactions producing osmium(II) complexes were established earlier for the reaction of the dioxo(porphyrino)osmium(VI) complex OsO_2(OEP) (OEP = *o*ct*ae*thyl*p*orphyrine) with triphenylphosphane.[7]

One very noticeable feature in the preparation of **3** is that on treatment of **3** with PPh_3 in dry tetrahydrofuran or other organic solvents like acetone or toluene, no reaction takes place. This result leads to the conclusion that this reaction is catalysed by protic species. If this is true, complex **3** should react with PPh_3 in protic solvents, e.g. alcohols. Hence, **3** was treated with PPh_3 in a methanolic medium and **5** was indeed produced, however, with an isolated yield of only 15%. This can be explained by the fact that MeOH can act as σ-donating ligand to the osmium centre, which might reduce the selectivity of the reaction of **3** with PPh_3 (vide supra). The need for the protic solvent for the reaction of **3** with **4** to produce **5**, indicates that the mechanism for this reaction may also include the protonation of the central O=Os=O building block, thus the oxo atoms in **3** would exchange with H_2O by protonation. The IR- and NMR-spectroscopic data of **5** agree with the structure found by X-ray crystal structure analysis (see below).

In the IR spectrum of **3**, a strong N−H stretching vibration is found, whereas in the IR spectrum of **5**, a broad $\nu_{(NH)}$ absorption band centred at around 3100 cm^{-1} is characteristic. The strong $\nu_{a(NO3)}$ vibration found at 1488 cm^{-1} in **3** is significantly shifted to lower frequencies in **5**, and is observed at 1384 cm^{-1}. These observations point to the formation of hydrogen bonds between the NH groups of the 2,2′-biimidazole building blocks, the oxygen atoms of the NO_3^- counter ions, the MeOH and the H_2O molecules.

As result of the reduction of osmium(VI) in **3** by PPh_3, the linear O=Os=O group in **3** is transferred to a zigzag $Ph_3P=O \rightarrow Os \leftarrow O=PPh_3$ unit in **5**. As a result, the $\nu_{a(Os=O)}$ absorption band found in the IR spectrum of **3** at 858 cm^{-1} is not present in the spectrum of **5**. Nevertheless, the disappearance of $\nu_{(Os=O)}$ is accompanied with the appearance of the P=O stretching vibrations at 1131 cm^{-1} in the IR spectrum of **5**.

In the ^1H NMR spectrum of **5** a multiplet between $\delta = 7.0$ and 8.2 is observed, resulting from the superimposition of the resonance signals of the protons of the phenyl groups, as well as the protons of the 2,2′-biimidazole chelating ligands. The $^{13}C\{^1H\}$ NMR spectrum of **5** shows the four resonance signals expected for the sp^2-hybridised phenyl carbon atoms of the $Ph_3P{=}O$ entities, between δ = 129 and 133. The resonance signals of the H_2biim chelating ligands are shifted to a lower field, relative to **3**, and are observed at δ = 135.1 (5,5′-position), δ = 137.9 (4,4′-position) and δ = 139.9 (2,2′-position), respectively.

$^{31}P\{^1H\}$-NMR-spectroscopic studies carried out on **5** clearly demonstrate the appearance of one resonance signal for the phosphorus atom of the triphenylphosphane oxide at δ = 36.4. Relative to the noncoordinated $Ph_3P{=}O$, the signal is shifted to a lower field by 9.4 ppm, revealing the coordination to the osmium(III) centre through the oxygen atom. Similar observations were made for other complexes featuring the P=O group, e.g. $[(\eta^5\text{-}C_5H_5)Co\{O{=}P(OR)_3\}_3]^-$ (R = Me, Ph).[8] The absorbance bands at 360 nm ($\varepsilon = 3.5 \cdot 10^3$ $mol^{-1} \cdot dm^3 \cdot cm^{-1}$) and 388 nm ($\varepsilon = 3.5 \cdot 10^3$ $mol^{-1} \cdot dm^3 \cdot cm^{-1}$) in the UV/Vis spectrum of **5** can be attributed to ligand-to-metal charge-transfer transitions.[9]

Complex **5** possesses a total of four NH functionalities, which can be easily deprotonated using KOH as a suitable base. Thus, the reaction of **5** with KOH in a molar ratio of 1:2 leads, on loss of KNO_3 and H_2O to the formation of the monocationic complex $[Os(Hbiim)_2(O{=}PPh_3)_2]NO_3$ (**6**) (Scheme 3). This reaction is accompanied by a colour change from red (**5**) to violet (**6**). After appropriate workup, **6** can be isolated in a 85% yield.

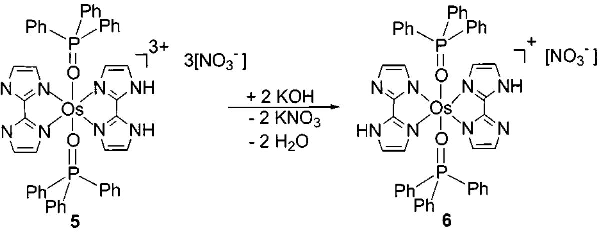

Scheme 3

A very noticeable feature in the IR spectrum of **6**, when compared with those of **3** and **5**, is the significant decrease in the intensity of the absorption bands of the NH and NO_3^- groups relative to the other vibrations observed in the spectrum. These absorptions are found at 3095 (NH) and 1386 cm^{-1} (NO_3^-), respectively. This result gives the first hint that the NH units of the 2,2′-biimidazole ligands could be at least partly metallated. This deprotonation influences the donor/acceptor properties of the 2,2′-biimidazole ligands, resulting in a change of the electronic absorbance in the UV/Vis spectrum of **6**. In contrast to **5**, the UV/Vis spectrum of **6** contains two maxima at 344 and at 541 nm, respectively.

All other spectroscopic studies carried out on **6** (^1H, $^{13}C\{^1H\}$ NMR spectroscopy) do not show a significant influence on the chemical shifts of the organic ligands when compared with **5**. However, the $^{31}P\{^1H\}$-NMR-spectroscopic studies demonstrate that on extended measurements further resonance signals appear. This can be attributed to ligand exchange reactions obtained by substitution of $O{=}PPh_3$ by solvent molecules, e.g. CD_3OD. As a result, signals with lower intensity are observed at δ = 33.7 ($Ph_3P{=}O{\rightarrow}Os{\leftarrow}DOMe$) and δ = 22.3 (*non*coordinated $Ph_3P{=}O$), next to the resonance signal at δ = 37.1 which is typical for **6**.

Electrochemical Studies

Cyclic voltammetric studies were carried out on complex **5** in dichloromethane at 25 °C and at −5 °C. The obtained voltammograms are depicted in Figure 1. However, due to the low solubility of **3** (vide supra) no electrochemical studies could be carried out on this complex for comparison. Figure 1 shows cyclic voltammograms of $[Os(H_2biim)_2(O{=}PPh_3)_2](NO_3)_3$ (**5**) in dichloromethane at 25 °C (top) and at −5 °C (bottom) (scan rate 60 mV s^{-1}).

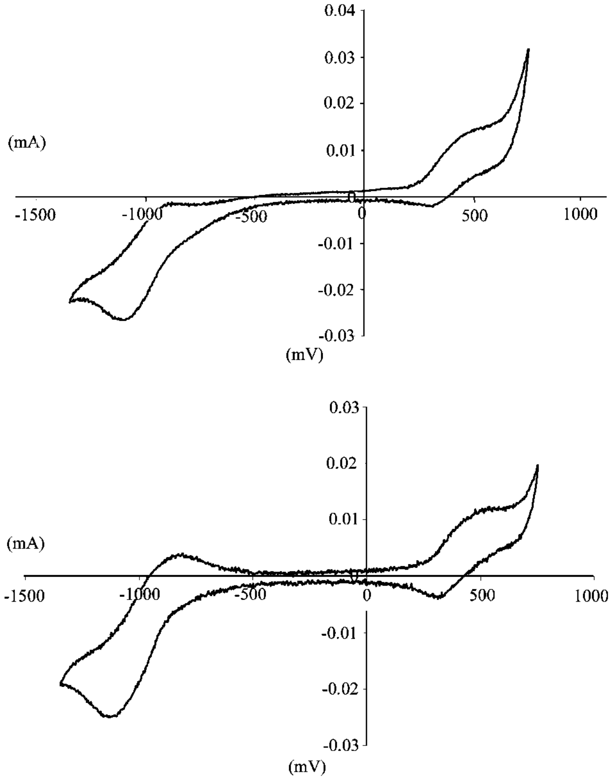

Figure 1. Cyclic voltammograms of $[Os(H_2biim)_2(O{=}PPh_3)_2](NO_3)_3$ (**5**) in dichloromethane at 25 °C (top) and at −5 °C (bottom) (scan rate 60 mV s^{-1})

It was found that both the Os^{III}/Os^{II} reduction (E_{red} = −1.09 V) and the Os^{III}/Os^{IV} oxidation processes (E_{ox} = +0.52 V) are irreversible at 25 °C. However, on lowering the temperature to −5 °C these processes are quasi-reversible. Thus, the potentials of the redox couples Os^{IV}/Os^{III} ($E_{1/2}$ = −0.97 V, ΔE = 290 mV) and Os^{IV}/Os^{V} ($E_{1/2}$ = +0.42 V, ΔE = 210 mV) could be determined. Similar observations were made for the Os^{IV} complex anion $[OsCl_5(H_2O)]^-$,[10] thus indicating that a reversible redox behaviour is seen only at low temperatures. This is a characteristic feature for some osmium complexes.[11] This can be explained by the kinetic stabilisation of the reactive intermediates e.g. the dicationic Os^{II} complex $[Os(H_2biim)_2(O{=}$

$PPh_3)_2]^{2+}$ at low temperatures. This species is produced by the electrochemical reduction of **5** and can be chemically oxidised by the NO_3^- ion. Decreasing temperatures slow down this reaction and lead to the formation of the anodic peak in the cyclic voltammogram, due to the electrochemical oxidation of the corresponding Os^{II} species.

A characteristic feature of the electrochemical behaviour of complex **6** is a significant shift of the redox potentials of the Os^{III}/Os^{IV} and Os^{III}/Os^{II} couples to a more negative value, relative to **5**. This results from a partial deprotonation of the H_2biim chelating ligands, followed by an increase in the electronic density on the appropriate osmium centre in **6**. In contrast to **5**, the shape of the cyclic voltammogram of **6** is temperature independent. Both at 25 °C and at −5 °C, the half potential of the Os^{III}/Os^{IV} redox couple is observed at +0.29 V. However, the Os^{III}/Os^{II} redox process is irreversible with $E_{red} = -1.29$ V.

Solid-State Structure of 5

Single crystals of **5**, suitable for X-ray structure analysis, were obtained by slow evaporation of a 1:1 methanol/dichloromethane solution at 25 °C. Complex **5** crystallises with two molecules of the complex, one molecule of water and half a molecule of methanol per asymmetric unit in the triclinic space group $P\bar{1}$, with $a = 10.9098(13)$, $b = 10.9726(12)$, $c = 21.330(3)$, $\alpha = 78.280(2)$, $\beta = 87.315(2)$, $\gamma = 87.992(2)°$, $V = 2496.6(5)$ Å^3 and $Z = 1$. Each of the complex molecules possesses a centre of inversion located at the osmium atom (Figure 2); the symmetry-generated atoms are indicated with the suffixes a and b. The molecular structure of **5** is shown in Figure 2. Experimental crystal data are listed in Table 3 and geometric details are presented in Table 1. Figure 2 shows a ZORTEP drawing of one complex cation $[Os(H_2biim)_2(O{=}PPh_3)_2]^{3+}$ of **5** (50% probability level; the second cation, NO_3^-, H_2O, and MeOH are omitted for clarity).

Each individual complex cation $[Os(H_2biim)_2(O{=}PPh_3)_2]^{3+}$ (Figure 2) of **5** possesses an osmium(III) centre in an octahedral environment, with two datively bonded $O{=}PPh_3$ units in the axial positions and two H_2biim chelating ligands in the equatorial positions. Complex **5** is the first example of an osmium(III) complex with two axial $O{=}PPh_3$ ligands. Similar complexes are known for osmium(II) and osmium(IV) systems, e.g. $Os(OEP)(O{=}PPh_3)_2$ (OEP = octaethylporphyrine)[7a] and $K_2[\{Os(\eta^4\text{-chba-Et})(O{=}PPh_3)_2\}_2O]$ [chba-Et = 1,2′-bis(3,5-dichloro-2-hydroxybenzaimido)ethane].[12]

The H_2biim arrangement in **5** is thereby planar (r. m. s. deviation of the fitted atoms Os1, N1 to N4, and C1 to C6 = 0.072 Å, as well as Os2, N5 to N8, and C25 to C30 = 0.085 Å). The angles around the osmium centres in the latter entity deviate from an idealised square-planar geometry [N1−Os1−N4 = 77.14(8)°, N5−Os2−N8 = 77.70(8)°], due to the formation of a five-membered OsN_2C_2 cycle. This value is typical for transition metal biimidazole complexes in which bite angels of 75.3° $\{[NEt_4][Ir(COD)(PPh_3)(tcbiim)]\cdot CH_2Cl_2$ (tcbiim = tetracyanobiimidazole)$\}$[13] and 82.78° $\{[Cu_2(Me_5dien)_2(biim)][BPh_4]_2$ (Me_5dien = pentamethyldiethylentriamine)$\}$[14] are found. A similar bite angle as observed in **5** was experimentally observed in $Ir_2(COD)_2(CH_3C{\equiv}N)(tcbiim)$ (78.214°).[14] Furthermore, this N−Os−N angle induces a distortion in the other angles of the equatorial square plane (Table 1).

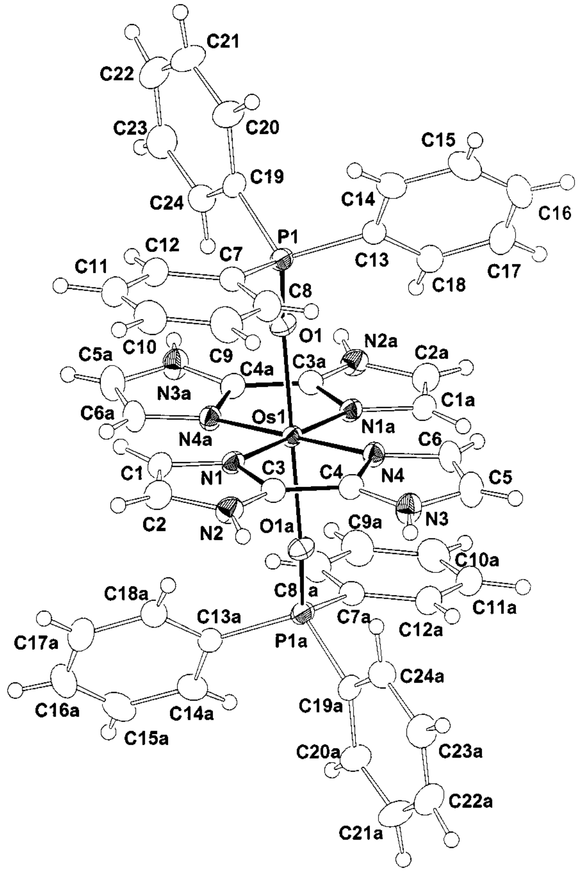

Figure 2. ZORTEP drawing of one complex cation $[Os(H_2biim)_2(O{=}PPh_3)_2]^{3+}$ of **5** (50% probability level; the second cation, NO_3^-, H_2O, and MeOH are omitted for clarity)

The two axially positioned $O{=}PPh_3$ ligands complete the octahedral coordination around the osmium atoms (for N−Os−O angles see Table 1). The Os−O−P angles of 146.53(11)° (Os1−O1−P1) and 140.16(11)° (Os2−O2−P2) are smaller than those found in $Os(OEP)(O{=}PPh_3)_2$ [154.2(5)°][7] and $K_2[\{Os(\eta^4\text{-chba-Et})(O{=}PPh_3)_2\}_2O]$ (153.0),[12] but still in the range typical for this type of arrangements. In general, M−O−P angles in $L_nM{-}O{=}PPh_3$ complexes (L_nM = transition metal fragment) range from 140 to about 180°, depending on the nature of the metal.[15]

The Os−O distances in **5** are 2.0129(16) Å (Os1−O1) and 2.0365(16) Å (Os2−O2), in between that found in $K_2[\{Os(\eta^4\text{-chba-Et})(O{=}PPh_3)_2\}_2O]$ (1.971 Å)[12] and $Os(OEP)(O{=}PPh_3)_2$ [2.036(7) Å].[7] This observation corresponds with the different ionic radii of Os^{II}, Os^{III}, and Os^{IV}.[5] The Os−N bonds, Os1−N1 [2.065(2) Å], Os1−N4 [2.072(2) Å], Os2−N5 [2.060(2) Å], and Os2−N8 [2.067(2) Å] are longer than the interatomic Os−N distances in the above-mentioned osmium complexes containing N ligands

Table 1. Selected geometrical details of $[Os(H_2biim)_2(O{=}PPh_3)_2](NO_3)_3{\cdot}H_2O{\cdot}0.5CH_3OH$ (**5**)

Bond lengths [Å][a] Molecule 1		Molecule 2	
Os1−O1	2.0129(16)	Os2−O2	2.0365(16)
Os1−N1	2.0651(19)	Os2−N5	2.060(2)
Os1−N4	2.072(2)	Os2−N8	2.067(2)
P1−O1	1.5195(17)	P2−O2	1.5224(18)
N1−C1	1.388(3)	N5−C25	1.375(3)
N2−C2	1.371(3)	N6−C26	1.372(4)
N1−C3	1.346(3)	N5−C27	1.355(3)
N2−C3	1.336(3)	N6−C27	1.329(3)
N3−C4	1.336(3)	N7−C28	1.337(3)
N3−C5	1.369(3)	N7−C29	1.373(4)
N4−C4	1.341(3)	N8−C28	1.344(3)
N4−C6	1.377(3)	N8−C30	1.379(3)
C1−C2	1.358(4)	C25−C26	1.358(4)
C3−C4	1.432(3)	C27−C28	1.432(3)
C5−C6	1.353(4)	C29−C30	1.346(4)
Bond angles [°] Molecule 1		Molecule 2	
O1−Os1−N1	94.13(7)	O2−Os2−N5	92.87(7)
O1−Os1−N1a	85.87(7)	O2−Os2−N5b	87.13(7)
O1−Os1−N4	97.61(7)	O2−Os2−N8	95.47(7)
O1−Os1−N4a	82.39(7)	O2−Os2−N8b	84.53(7)
N1−Os1−N4	77.14(8)	N5−Os2−N8	77.70(8)
P1−O1−Os1	146.53(11)	P2−O2−Os2	140.16(11)

[a] Symmetry transformations used to generate equivalent atoms: *a* = −*x* + 1, −*y* + 1, −*z*; *b* = −*x*, −*y*, −*z* + 1.

and triphenylphosphane oxide, but significantly shorter than those found in osmium complexes featuring the H_2biim ligand and phosphanyl groups, e.g. $[OsCl(\eta^2\text{-}H_2)(H_2biim)(PiC_3H_7)_2]Cl$ (2.110−2.135 Å).[4a]

Figure 3 shows the SCHAKAL-99 drawing of **5** including the hydrogen-bonding scheme (phenyl groups of the $O{=}PPh_3$ ligands are omitted for clarity). As depicted in Figure 3, complex **5** possesses a polymeric zigzag chain in the solid state, due to hydrogen bonds between the complex cations $[Os(H_2biim)_2(O{=}PPh_3)_2]^{3+}$, NO_3^-, and the neutral solvent molecules H_2O and MeOH. The corresponding interatomic distances for all specified hydrogen bonds are presented in Table 2 and are in accordance with typical bond lengths between donor and acceptor atoms forming hydrogen bonds.[16] The complex cations in **5** (Figure 3) are spanned by two different linking units: (i) NO_3^- and (ii) NO_3^- and H_2O. However, the H_2O molecule of the latter building arrangement gives rise to a further hydrogen bond with the third NO_3^- ion, which itself is hydrogen-bonded to a terminal MeOH moiety (Figure 3).

Table 2. Specified hydrogen bonds in $\mathbf{5}{\cdot}H_2O{\cdot}0.5MeOH$

Atoms[a]			Interatomic distances [Å]			Angles [°]
D	H	A	D−H	H−A	D−A	D−H−A
N2	H1N2	O8	0.82(3)	1.98(3)	2.795(3)	173(3)
N3	H1N3	O4c	0.85(3)	1.98(3)	2.788(3)	161(3)
N6	H1N6	O6d	0.84(3)	1.90(3)	2.733(3)	171(3)
N7	H1N7	O12e	0.84(3)	1.87(4)	2.680(3)	161(3)
O12	H112	O10	0.78(4)	2.00(4)	2.767(4)	167(4)
O12	H113	O3	0.78(4)	2.12(4)	2.794(3)	145(4)
O12	H113	O6f	0.78(4)	2.50(4)	2.971(3)	120(4)
O13	H13	O9	0.84	2.15	2.918(9)	152.6

[a] D = Donor, H = Hydrogen, A = Acceptor; symmetry transformations used to generate equivalent atoms: *c* = *x* − 1, *y*, *z*; *d* = *x*, *y* − 1, *z*; *e* = *x* − 1, *y* − 1, *z*; *f* = *x* + 1, *y*, *z*.

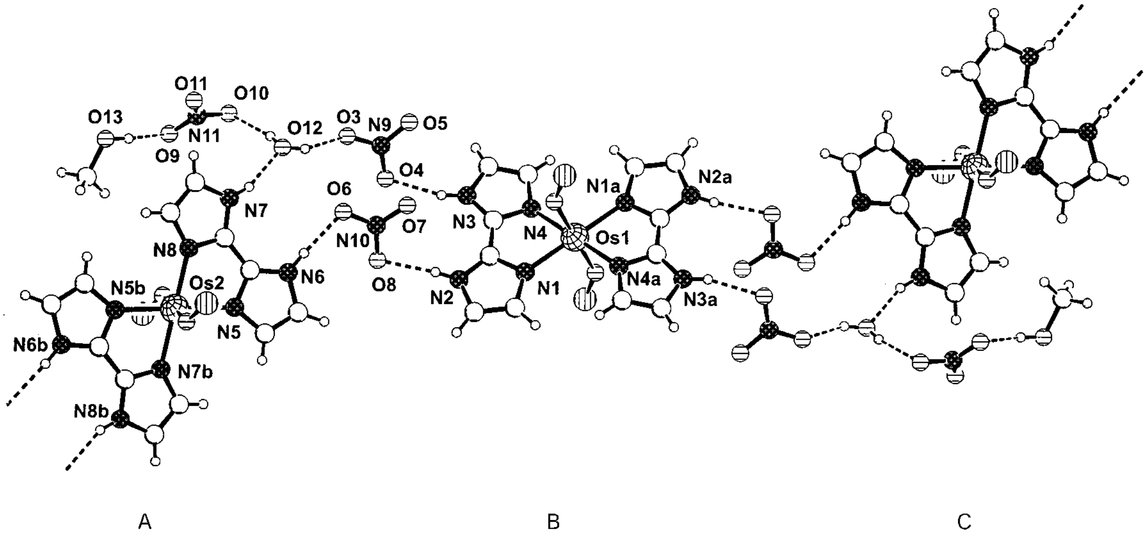

Figure 3. SCHAKAL-99 drawing of **5** including the hydrogen-bonding scheme (phenyl groups of the $O{=}PPh_3$ ligands are omitted for clarity)

Conclusions

In this study, it is shown that novel osmium complexes, featuring two 2,2′-biimidazole ligands are easily accessible. In addition, the novel dioxoosmium(VI) complex $[OsO_2(H_2biim)_2](NO_3)_2$ (**3**) is a very useful precursor for the preparation of an osmium(III) complex, $[Os(H_2bim)_2(O{=}PPh_3)_2](NO_3)_3$ (**5**), on reaction with PPh_3 in the presence of HNO_3. This reaction involves the transfer of an oxygen atom from osmium to phosphorus, and hence redox processes are typical. Furthermore, complex **5** can be deprotonated, with KOH as a suitable base, to afford monocationic $[Os(Hbiim)_2(O{=}PPh_3)_2](NO_3)$ (**6**). Complexes **5** and **6** both possess an osmium centre in an octahedral environment, as a result of the two 2,2′-biimidazole chelating ligands which are in the equatorial positions and two triphenylphosphane oxide groups in the axial positions *trans* to each other.

In future studies, the use of the latter complexes in the preparation of oligometallic complexes is of interest, since they bear with their 2,2′-biimidazole ligands coordination sites for the addition of further transition metal building blocks. These accessible complexes should provide very promising model systems for the study of electron transfer reactions and, in addition, they should be excellent catalysts in homogeneous catalysis due to the synergistic and cooperative effects of further transition metals being present.

Experimental Section

General Remarks: IR spectra were recorded with a Perkin−Elmer FT-IR spectrometer (Spectrum 1000) as KBr pellets. − UV/Vis spectra were recorded with a Perkin−Elmer Lambda 40 spectrophotometer in dichloromethane solutions and the concentrations were $8.0{\cdot}10^{-5}$ $mol{\cdot}dm^{-3}$. − NMR spectra were recorded with a Bruker Avance 250 spectrometer, operating in the Fourier transform mode; NMR spectra were recorded at 250.131 MHz (^1H), 62.902 MHz ($^{13}C\{^1H\}$) or 101.249 MHz ($^{31}P\{^1H\}$, $T = 303$ K); chemical shifts (δ) are given in ppm with respect to $CDCl_3$ (^1H: $\delta = 7.29$; $^{13}C\{^1H\}$: $\delta = 77.5$) as an internal standard. ^{31}P chemical shifts (δ) are given in ppm with respect to 85% H_3PO_4 (^{31}P: $\delta = 0$) and $P(OMe)_3$ ($\delta = 139$) as an external standard. − Melting (decomposition) points were determined with a Gallenkamp MFB 595 010 M melting point apparatus. − Electrochemical measurements were performed by cyclic voltammetry in dichloromethane solutions containing $[nBu_4N]PF_6$ (0.1 $mol{\cdot}dm^{-3}$) at 25 °C and at −5 °C, using a standard three-electrode Pt−Pt−calomel cell and a Radiometer DEA 101 potentiostat. A scan rate of 60 $mV{\cdot}s^{-1}$ was used. All potentials were referenced to the ferrocene/ferrocenium FcH/Fc^+ couple ($E_{1/2} = 0.000$ V). − Organic solvents (methanol, acetone, tetrahydrofuran, dichloromethane, CCl_4) were freshly distilled before use. Commercially available triphenylphosphane was used without further purification. 2,2′-Biimidazole was synthesised according to a literature procedure.[17] − Microanalyses were performed by the Laboratory of Elemental Analysis of the Technische Universität Bergakademie Freiberg.

Synthesis of $[OsO_2(H_2biim)_2](NO_3)_2{\cdot}CH_3OH$ (3): OsO_4 (**1**) (0.75 mmol, 5 mL of a 0.15 M solution), in CCl_4 was added to 40 mL of a 1:1 methanol/acetone mixture, containing H_2biim (**2**) (250 mg, 1.87 mmol) and HNO_3 (2.0 mmol) at 25 °C. The reaction mixture was heated to reflux for 4 h, and an orange product precipitated. After the reaction mixture was cooled to 25 °C, the orange precipitate was filtered, washed with 20 mL of acetone and dried in an oil-pump vacuum to afford **3**. Yield: 290 mg (0.45 mmol), 60% based on OsO_4. − M.p. gradual decomposition at $T > 150$ °C. − IR (KBr, cm^{-1}): $\nu_{a(Os=O)}$ 858, $\nu_{a(NO_3^-)}$ 1488, $\nu_{(NH)}$ 3140. − ^1H NMR ($[D_6]$DMSO): $\delta = 7.8$ (br. s, 4 H, 5- ,5′-H/H_2biim), 8.5 (br. s, 4 H, 4- ,4′-H/H_2biim). − $^{13}C\{^1H\}$ NMR ($[D_6]$DMSO): $\delta = 123.4$ (C-5, -5′/H_2bim), 128.7 (C-4, -4′/H_2biim). − Due to the low solubility of **3**, no further resonance signals could be detected. − $C_{13}H_{16}N_{10}O_9Os$ (646.54): calcd. C 24.15, H 2.50; N 21.67; found C 24.19, H 3.00, N 22.63.

Synthesis of $[Os(H_2biim)_2(O{=}PPh_3)_2](NO_3)_3{\cdot}H_2O{\cdot}0.5CH_3OH$ (5): $[OsO_2(H_2biim)_2](NO_3)_2{\cdot}CH_3OH$ (**3**) (200 mg, 0.31 mmol) was suspended in 50 mL of tetrahydrofuran (10% H_2O) containing PPh_3 (**4**) (175 mg, 0.665 mmol). The reaction mixture was heated to reflux for 3 h. HNO_3 (0.6 mL of a 0.5 M solution) was then added and the solution immediately turned from brown to red. The solution was cooled to 25 °C and filtered through a glass filter. All volatiles were then removed in an oil-pump vacuum. The remaining red residue was washed several times with 20 mL of toluene and 20 mL of dry tetrahydrofuran, and was then dried in vacuo to give a crude red product, which was crystallised from a dichloromethane/methanol mixture (4:1) at 25 °C to afford **5** as red crystals. Yield: 290 mg (0.23 mmol), 76% based on **3**. − M.p. 189 °C (dec.). − IR (KBr, cm^{-1}): $\nu_{a(NO_3)}$ 1385, $\nu_{(NH)}$ 3106, $\nu_{(P=O)} = 1131$. − ^1H NMR ($[D_6]$DMSO): $\delta = 7.0{-}8.2$ (m, C_6H_5, H_2biim). − $^{13}C\{^1H\}$ NMR ($[D_6]$DMSO): $\delta = 129.1$ (C-*i*/C_6H_5), 130.2 (CH/C_6H_5), 131.8 (CH/C_6H_5), 133.0 (CH/C_6H_5), 135.1 (C-5, -5′/H_2biim), 137.9 (C-4, -4′/H_2biim), 139.9 (C-2, -2′/H_2bim). − $^{31}P\{^1H\}$ NMR ($[D_6]$DMSO): $\delta = 36.4$. − UV/Vis (CH_2Cl_2): $\lambda_{max} = 360$ nm ($\varepsilon = 3.5{\cdot}10^3$ $mol^{-1}{\cdot}dm^3{\cdot}cm^{-1}$), 388 nm ($\varepsilon = 3.5{\cdot}10^3$ ($mol^{-1}{\cdot}dm^3{\cdot}cm^{-1}$). − CV ($CH_2Cl_2$, −5 °C): Os^{III}/Os^{II} redox couple, $E_{1/2} = -0.97$ V ($\Delta E = 290$ mV), Os^{III}/Os^{IV} redox couple, $E_{1/2} = +0.42$ V ($\Delta E = 210$ mV). − $C_{48}H_{48}N_{11}O_{12}OsP_2$ (1236.20): calcd. C 47.12, H 3.84, N 12.47; found C 47.36, H 4.19, N 12.11.

Synthesis of $[Os(Hbiim)_2(O{=}PPh_3)_2](NO_3){\cdot}2H_2O$ (6): Potassium hydroxide (30 mg, 0.53 mmol, dissolved in 5 mL of methanol) was added to a solution of $[Os(H_2bim)_2(O{=}PPh_3)_2]$-$(NO_3)_3{\cdot}H_2O{\cdot}0.5CH_3OH$ (**5**) (300 mg, 0.26 mmol) in a 4:1 dichloromethane/methanol mixture at 25 °C. The reaction mixture immediately turned from red to violet and KNO_3 subsequently precipitated. The reaction mixture was additionally stirred for 20 min and then filtered through a glass filter. From the filtrate all volatiles were removed in an oil-pump vacuum. The violet residue was washed with 10 mL of H_2O, 5 mL of acetone, and then dried in vacuo to afford **6** as a violet solid. Yield: 240 mg (0.22 mmol), 85% based on **5**. − M.p. 226 °C (dec.). − IR (KBr, cm^{-1}): $\nu_{a(NO_3)}$ 1386, $\nu_{(NH)}$ 3095, $\nu_{(P=O)}$ 1132. − ^1H NMR ($[D_4]$methanol): $\delta = 7.4{-}8.1$ (m, C_6H_5, H_2biim). − $^{13}C\{^1H\}$ NMR ($[D_4]$methanol): $\delta = 130.5$ (CH/C_6H_5), 133.4 (CH/C_6H_5), 133.6 (CH/C_6H_5), 134.6 (C-5, -5′/H_2biim), 138.6 (C-4, -4′/H_2biim), 141.3 (C-2, -2′/H_2bim). − Due to the low solubility of **6** the C-*i*/C_6H_5 resonance signal could not be detected. − $^{31}P\{^1H\}$ NMR ($[D_6]$DMSO): $\delta = 37.1$. − UV/Vis (CH_2Cl_2): $\lambda_{max} = 341$ nm ($\varepsilon = 4.5{\cdot}10^3$ $mol^{-1}{\cdot}dm^3{\cdot}cm^{-1}$), 541 nm ($\varepsilon = 4.5{\cdot}10^2$ ($mol^{-1}{\cdot}dm^3{\cdot}cm^{-1}$). − CV ($CH_2Cl_2$, 25 °C): Os^{III}/Os^{II} redox couple, $E_{red} = -1.29$ V (irr.); Os^{III}/Os^{IV} redox couple, $E_{1/2} = +0.29$ V ($\Delta E = 180$ mV). − $C_{48}H_{44}N_9O_6OsP_2$ (1095.15): calcd. C 52.64, H 4.06, N 11.51; found C 52.82, H 3.89, N 12.11.

X-ray Crystallographic Study of 5: X-ray structure data (total/unique reflections: 20917/13900) were collected at 170 K with a

Bruker SMART CCD diffractometer for the red crystals of **5** (Table 3). The crystal was attached to a glass fiber with perfluoropolyalkyl ether (ABCR GmbH & Co KG, viscosity 1600 cSt.). The unit cell parameter was checked for the presence of higher lattice symmetry using PLATON.[18] Data were corrected for absorption using SADABS.[19] The structure was solved by direct methods (SHELXS-97).[20] Refinement was carried out by full-matrix least-squares techniques on F^2 (SHELXL-97/2).[20] Hydrogen atoms were located from the difference Fourier map. All hydrogen atoms were fully refined with the exception of H13, H49a, H49b, and H49c, which belong to the CH_3OH molecule and were included on their ideal positions, riding on their carrier atoms. All non-hydrogen atoms were refined anisotropically. The structural data (without structural factors) are deposited at the Cambridge Crystallographic Data Centre and can be acquired under the depositing number CCDC-152194 under the following address: CCDC, 12 Union Road, Cambridge CB2 1EZ, UK [Fax: (internat.) + 44-1223/336-033; E-mail: deposit@ccdc.cam.ac.uk].

Table 3. Crystallographic data for $\mathbf{5}\cdot H_2O\cdot 0.5MeOH$

Crystal shape	plate
Crystal colour	red
Crystal size [mm]	1.00 × 0.40 × 0.10
Empirical formula	$C_{97}H_{92}N_{22}O_{25}Os_2P_4$
Molecular mass	2470.21
Crystal system	triclinic
Space group	$P\bar{1}$
a [Å]	10.9098(13)
b [Å]	10.9726(13)
c [Å]	21.330(3)
α [°]	78.280(2)
β [°]	87.315(2)
γ [°]	87.992(2)
V [Å^3]	2496.6(5)
Z	1
$d_{\mathrm{calcd.}}$ [g·cm^{-3}]	1.643
Type of diffractometer	Bruker SMART CCD
Radiation used (λ [Å])	Mo-K_α (0.71073)
Monochromator	graphite
Data collection mode	ω-scans
Linear absorption coefficient [mm^{-1}]	2.694
Temperature [K]	173(2)
Max/Min transmission	0.7744/0.1737
Number of measured reflections	20917
Number of independent reflections	13900
Unique reflections ($I \geq 2\sigma(I)$]	10155
R(int)	0.0224
Scan range	$0.98° \leq \theta \leq 30.87°$
Completeness to $\theta_{\max}$	98.3%
Index range	$-15 \leq h \leq 15$
	$-15 \leq k \leq 15$
	$-29 \leq l \leq 19$
F(000)	1240
R [$I > 2\sigma(I)$]/all[a]	0.0245/0.0388
wR^2 [$I > \sigma(I)$]/all[b]	0.0581/0.0626
Maximum δ/σ	1.444
Max./min. electron density [e·Å^{-3}]	1.176/−1.333
Reflections used for refinement	13900
Refined parameters	863
Goodness-of-fit on F^2 [c]	0.983

[a] $R = \Sigma||F_o| - |F_c||/\Sigma|F_o|$. − [b] $[\Sigma[w(F_o^2 - F_c^2)^2]/\Sigma(wF_o^4)]^{1/2})$, calcd. $w = 1/[\sigma^2(F_o^2) + (0.0339P)^2 + 0.0000P]$ where $P = (F_o^2 + 2F_c^2)/3$. − [c] $S = [\Sigma w(F_o^2 - F_c^2)2]/(n - p)^{1/2}$, n = number of reflections, p = parameters used.

Acknowledgments

This work was supported in part by the Deutsche Forschungsgemeinschaft, the Fonds der Chemischen Industrie and the Deutscher Akademischer Austauschdienst DAAD (A. M.). We also would like to thank Degussa-Hüls AG for the generous gift of OsO_4 and $OsCl_3$.

---

[1] [1a] L. A. Oro, E. Sola, J. A. López, F. Torres, A. Elduque, F. Lahoz, *Inorg. Chem. Commun.* **1998**, *1*, 64−67. − [1b] C. Tejel, M. A. Ciriano, J. A. López, F. J. Lahoz, L. A. Oro, *Organometallics* **1997**, *16*, 4718−4727. − [1c] P. G. Rasmussen, J. E. Anderson, O. H. Bailey, M. Tamres, J. C. Bayón, *J. Am. Chem. Soc.* **1985**, *107*, 279−281. − [1d] P. G. Rasmussen, O. H. Bailey, J. C. Bayón, W. M. Butler, *Inorg. Chem.* **1984**, *23*, 338−343.

[2] [2a] L. A. Oro, M. A. Ciriano, C. Tejel, *Pure Appl. Chem.* **1998**, *70*, 779−788. − [2b] E. Sola, V. I. Bakhmutov, F. Torres, A. Elduque, J. A. López, F. J. Lahoz, H. Werner, L. A. Oro, *Organometallics* **1998**, *17*, 683−696. − [2c] M. A. Esteruelas, M. P. Garcia, A. M. Lopez, L. A. Oro, *Organometallics* **1992**, *11*, 702−705. − [2d] M. P. Garcia, A. M. Lopez, M. A. Esteruelas, F. J. Lahoz, L. A. Oro, *J. Chem. Soc., Chem. Commun.* **1988**, 793−795.

[3] M. A. Esteruelas, M. P. García, A. M. López, L. A. Oro, *Organometallics* **1991**, *10*, 127−133.

[4] [4a] M. A. Esteruelas, F. J. Lahoz, L. A. Oro, E. Onate, N. Ruiz, *Inorg. Chem.* **1994**, *33*, 787−792. − [4b] M. A. Esteruelas, F. J. Lahoz, A. Lopez, E. Onate, L. A. Oro, N. Ruiz, E. Sola, J. Tolosa, *Inorg. Chem.* **1996**, *35*, 7811−7817.

[5] W. P. Griffith, Osmium, *Comprehensive Coordination Chemistry*, vol. 4 (Ed.: G. Wilkinson), Oxford, Pergamon Press, **1987**, p. 580−587.

[6] K. Nakamoto, *Infrared and Raman Spectra of Inorganic and Coordination Compounds*, John Wiley and Sons, Inc., NY, **1986**, p. 295−301.

[7] [7a] C. M. Che, T. F. Lai, W. C. Chung, W. P. Schaefer, H. B. Grey, *Inorg. Chem.* **1987**, *26*, 3907−3911. − [7b] C. M. Che, C. K. Poon, W. C. Chung, H. B. Grey, *Inorg. Chem.* **1985**, *24*, 1277−1278.

[8] [8a] B. Domhoever, H. Hammers, W. Klaeui, M. Pfeffer, *J. Organomet. Chem.* **1996**, *522*, 197−206. − [8b] B. Domhoever, W. Klaeui, *J. Organomet. Chem.* **1996**, *522*, 207−212. − [8c] W. Kläui, H. O. Asbah, G. Schramm, V. Englert, *Chem. Ber./Recueil* **1997**, *130*, 1223−1229.

[9] A. B. P. Lever, *Inorganic Electronic Spectroscopy*, Elsevier, Amsterdam, London, New York, **1968**, p. 225−236.

[10] A. Maiboroda, G. Rheinwald, H. Lang, *Inorg. Chem.* **2000**, *39*, 5725−5730.

[11] K. J. Taylor, L. J. Yellowlees, *Molecular Electrochemistry of Inorganic, Bioorganic and Organometallic Compounds, NATO ASI Ser., Ser. C.*, Kluwer Academic Publishers, Amsterdam, **1993**, p. 69−75.

[12] J. A. Christie, T. J. Collins, Terry E. Krafft, Bernard D. Santasiero, G. H. Spies, *J. Chem. Soc., Chem. Commun.* **1984**, 198−199.

[13] G. A. Jeffrey, H. Maluszynska, J. Mitra, *Int. J. Biol. Macromol.* **1985**, *7*, 336−348.

[14] P. G. Rasmussen, O. H. Bailey, J. C. Bayón, W. M. Butler, *Inorg. Chem.* **1984**, *23*, 338−343.

[15] M. S. Haddad, E. N. Duesler, D. N. Hendrickson, *Inorg. Chem.* **1979**, *18*, 141−148.

[16] *Comprehensive Organometallic Chemistry* (Eds. G. Wilkinson et al.), Pergamon Press, Oxford, **1982**, vol. 1−9.

[17] F. Holmes, K. M. Jones, E. G. Torrible, *J. Chem. Soc.* **1961**, 4790−4794.

[18] A. L. Spek, *Acta Crystallogr., Sect. A* **1990**, *46*, C34.

[19] Area Detector, *Absorption Corrections*, Bruker axs Inc., Madison, WI, **1996**.

[20] G. M. Sheldrick, *Shelx97, Programs for Crystal Structure Analysis (Release 97-2)*, University of Göttingen, Germany, **1997.**

Received December 8, 2000
[I00466]